Int. J. Heat Mass Transfer. Vol. 33, No. 5, pp. 827–833, 1990
Printed in Great Britain

0017–9310/90 $3.00 + 0.00

Natural convection in liquid-saturated porous media between concentric inclined cylinders

BU-XUAN WANG and XING ZHANG
Thermal Engineering Department, Tsinghua University, Beijing 100084, China

(*Received* 9 *March* 1989 *and in final form* 6 *July* 1989)

Abstract—Numerical studies are reported for three-dimensional steady natural convection in liquid-saturated porous media enclosed between concentric inclined cylinders. The inner cylinder is kept at constant heat flux or is isothermal, while the outer cylinder is kept isothermal and the end plates insulated. Numerical studies range for: Rayleigh number, $Ra \leqslant 10^3$; radius ratio, $1 \leqslant R_o \leqslant 10$; aspect ratio, $1 \leqslant A \leqslant 15$; angle of inclination, ϕ, from 0° to 90°. Numerical results show that, there exists a critical aspect ratio, for which the angle of inclination has no effect on the heat transfer. Good agreements between numerical results and experimental values have been ascertained for mean Nusselt number, Nu_m.

1. INTRODUCTION

NATURAL convection in porous annuli has been previously studied mostly for vertical and horizontal annuli. Only a few studies of natural convection in inclined porous annuli have been reported in the literature due to its complexity for three-dimensional flow. The three-dimensional natural convection in liquid-saturated porous media is important in numerous technological applications, including energy storage, heat pipes, geothermal systems and drying processes. Combarnous and Bories [1], Cheng [2] and Wang and Zhang [3] have provided reviews of the state-of-the-art on natural convection in liquid-saturated porous media. Three-dimensional natural convection heat transfer in inclined concentric annuli is a subject which needs urgent investigation. Takata *et al.* [4, 5] reported some results on such an investigation, but they studied only one geometrical size and missed out some terms in their mathematical model.

We had reported our investigations on transient and steady-state natural convection in vertical [3] and horizontal [6] liquid-saturated porous annuli. This paper reports work extended to study three-dimensional steady natural convection in an inclined liquid-saturated porous annulus for comparatively wide ranges of aspect ratio, radius ratio, angle of inclination, Rayleigh number, and the mutual effects of these parameters on flow and heat transfer. The predicted $Nu_{m,i}$ agreed quite well with measured values.

2. MATHEMATICAL FORMULATION

Consider a liquid-saturated porous medium bounded between two concentric inclined cylinders of radii r_i and r_o, respectively. The cylinders are impermeable, with the inner cylinder maintained at either constant uniform temperature, T_i, or constant uniform heat flux, q_i, and the outer cylinder maintained at constant uniform temperature, T_o, while both end walls are insulated. The configuration of the system is shown in Fig. 1. As a result of the temperature difference, fluid motion will be induced in the medium.

The governing equations for steady natural convection with the Boussinesq and Darcy flow approxi-

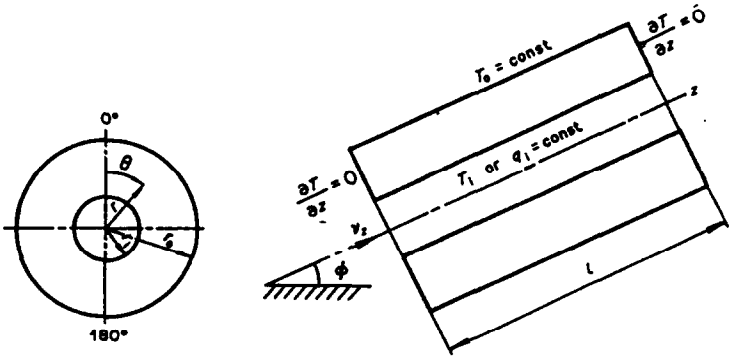

FIG. 1. Analytical model.

NOMENCLATURE

A	aspect ratio, $l/(r_o-r_i)$
c_p	specific heat at constant pressure
g	gravitational acceleration
Gr	Grashof number
K	permeability
l	axial length of annulus
Nu	Nusselt number
Nu_m	mean Nusselt number
Pr	Prandtl number
q	heat flux
r, z	coordinates
Ra	Rayleigh number
R_o	radius ratio, r_o/r_i
T	temperature
v	velocity vector
Z	z/r_i [dimensionless].

Greek symbols

β	coefficient of thermal expansion
ε	porosity
λ	thermal conductivity
μ	viscosity
ρ	density
ϕ	angle of inclination
ψ	stream function.

Subscripts

f	fluid
i	inner surface
o	outer surface.

mations are given as

$$\nabla\cdot\mathbf{v}=0 \tag{1}$$

$$-\nabla p+\mathbf{G}-(\mu/K)\mathbf{v}=0 \tag{2}$$

$$\lambda^*\nabla^2 T=\rho_f c_{p,f}\nabla\cdot(\mathbf{v}T) \tag{3}$$

$$\rho_f=\rho_o[1-\beta_f(T-T_o)]. \tag{4}$$

The apparent thermal conductivity, λ^*, is given as

$$\lambda^*=\varepsilon\lambda_f+(1-\varepsilon)\lambda_s \tag{5}$$

and the volumetric force vector, G, as

$$\mathbf{G}=\left[-\rho_f g\cos\theta\cos\phi,\ \rho_f g\sin\theta\cos\phi,\ -\rho_f g\sin\phi\right]\cdot\begin{vmatrix} r \\ \theta \\ z\end{vmatrix}$$

where v is the velocity vector, T the temperature, c_p the specific heat, K the permeability, ρ the density, μ the viscosity, ε the porosity, and β_f the thermal expansion coefficient of fluid, with subscripts 'f' and 's' the fluid and solid, respectively.

The stream function, ψ, is defined as

$$\mathbf{v}=\nabla\times\psi \quad\text{and}\quad \nabla\cdot\psi=0. \tag{6}$$

Using dimensionless variables, $R=r/r_i$, $Z=z/r_i$, $v_r=\lambda^*/(\rho_f l c_{p,f})$, $\Psi_r=\psi_r/(lv_r)$, $\Psi_\theta=\psi_\theta/(lv_\theta)$, $\Psi_z=\psi_z/(lv_z)$, and $\Theta=(T-T_o)/(T_i-T_o)$, then equations (1)–(4) can be transformed to the following dimensionless equations:

$$\nabla^2\Psi_r-\left[\frac{\Psi_r}{r^2}+\frac{2}{r^2}\frac{\partial\Psi_\theta}{\partial\theta}\right]=$$

$$-Ra\frac{r_i}{r_o-r_i}\left(\frac{\sin\phi}{R}\frac{\partial\Theta}{\partial\theta}+\frac{r_i}{l}\sin\theta\cos\phi\frac{\partial\Theta}{\partial Z}\right) \tag{7}$$

$$\nabla^2\Psi_\theta-\left[\frac{\Psi_\theta}{r^2}-\frac{2}{r^2}\frac{\partial\Psi_\theta}{\partial\theta}\right]=$$

$$Ra\frac{r_i}{r_o-r_i}\left(\sin\phi\frac{\partial\Theta}{\partial R}-\frac{r_i}{l}\cos\theta\cos\phi\frac{\partial\Theta}{\partial Z}\right) \tag{8}$$

$$\nabla^2\Psi_z=Ra\frac{l}{r_o-r_i}\left(\sin\theta\cos\phi\frac{\partial\Theta}{\partial\theta}\right) \tag{9}$$

$$\nabla^2\Theta=\frac{r_i}{l}\mathbf{v}\cdot\nabla\Theta \tag{10}$$

where

$$\nabla^2=\frac{\partial^2}{\partial R^2}+\frac{1}{R}\frac{\partial}{\partial R}+\frac{1}{R^2}\frac{\partial^2}{\partial\theta^2}+\frac{r_i^2}{l^2}\frac{\partial^2}{\partial Z^2}$$

and the Rayleigh number, Ra, is given as

$$Ra=Gr\,Pr=g\beta_f\rho_o\rho_f c_{p,f}(r_o-r_i)K(T_i-T_o)/(\lambda^*\mu). \tag{11}$$

These dimensionless equations also apply for the prescribed uniform heat flux at the inner cylinder surface, q_i, with the reference temperature difference defined as

$$(T_i-T_o)=q_i(r_o-r_i)/\lambda^*.$$

In such a case, the Rayleigh number based on heat flux will appear in equations (7)–(9), i.e.

$$Ra=g\beta_f\rho_o\rho_f c_{p,f}(r_o-r_i)^2Kq_i/(\lambda^{*2}\mu) \tag{12}$$

and the dimensionless temperature excess, $\Theta=(T-T_o)/(T_i-T_o)$, is given as

$$\Theta=\lambda^*(T-T_o)/[q_i(r_o-r_i)].$$

The relevant hydrodynamic boundary conditions

are

$$\left.\begin{aligned}\frac{\partial(R\Psi_r)}{\partial R} &= \Psi_\theta = \Psi_z = 0 \quad \text{at } R = 1 \text{ and } R_o \\ \frac{\partial(\Psi_\theta)}{\partial\theta} &= \Psi_r = \Psi_z = 0 \quad \text{at } \theta = 0 \text{ and } \pi \\ \frac{\partial(\Psi_z)}{\partial Z} &= \Psi_r = \Psi_\theta = 0 \quad \text{at } Z = 0 \text{ and } 1\end{aligned}\right\} \quad (13)$$

and the thermal boundary conditions are

$$\left.\begin{aligned}\Theta &= 1 \quad \text{at } R = 1 \\ \Theta &= 0 \quad \text{at } R = R_o \\ \frac{\partial\Theta}{\partial\theta} &= 0 \quad \text{at } \theta = 0 \text{ and } \pi \\ \frac{\partial\Theta}{\partial Z} &= 0 \quad \text{at } Z = 0 \text{ and } 1.\end{aligned}\right\}. \quad (14)$$

The local Nusselt numbers for the inner and outer cylinder surfaces are defined respectively as

$$Nu_i = \ln\frac{r_o}{r_i}\left.\frac{\partial\Theta}{\partial R}\right|_{R=1} \quad (15)$$

and

$$Nu_o = \left(\frac{r_o}{r_i}\right)\ln\frac{r_o}{r_i}\left.\frac{\partial\Theta}{\partial R}\right|_{R=R_o} \quad (16)$$

The mean Nusselt number at each surface is given by

$$Nu_{m,i} = \frac{1}{\pi}\int_0^1\int_0^1 Nu_i \, d\theta \, dZ \quad (17)$$

or

$$Nu_{m,o} = \frac{1}{\pi}\int_0^1\int_0^1 Nu_o \, d\theta \, dZ. \quad (18)$$

3. NUMERICAL CALCULATION

Finite differential equations are derived from equations (7) to (10) and solved by the method of successive over relaxation (SOR). The first and second derivatives were approximated by three-point central difference expressions, which have second-order accuracy.

To judge the iterative convergence of the solution, a criterion

$$[1-\zeta^{k-1}/\zeta^k]_{max} \leqslant \varepsilon_i \quad (19)$$

was used at every grid point for both Θ and the stream function, ψ. A suitable value for ε_i was taken as 10^{-3}, which provides enough convergence accuracy.

A mesh of $11 \times 19 \times 33$ was chosen for low Rayleigh numbers, and a mesh of $21 \times 37 \times 65$ was chosen for high Rayleigh numbers. Discussions for the effects of such mesh sizes, relaxation parameters, convergence criterion, etc. on accuracy and computational time are presented in ref. [7].

Numerical results have been obtained for: Ra, up to 10^3; aspect ratio, $A = l/(r_o - r_i)$, from 1 to 15; radius ratio, R_o $(= r_o - r_i)$, from 1 to 10; and angle of inclination, ϕ, from 0° to 90°.

It is clear that $v = 0$ at both ends and so the velocity and temperature distributions will differ with different cross-sections. Figure 2 shows the velocity distributions and isotherms $\Theta = 0, 0.2, 0.4, 0.6, 0.8$ and 1.0 at the mid-plane $(Z = 0.5)$ for three aspect ratios, from which we note that the aspect ratio, A, only effects velocity and temperature distributions at the mid-plane if it exceeds 4. Figure 3 shows that the isotherms shift towards the hot wall and so enhance heat transfer as R_o increases.

The predicted effects of Ra on Nu_i and Nu_o are given in Fig. 4, from which the effect of cylindrical coordinate θ and Z seems to be increased as Ra increases. The maximum value of Nu_i for the inner cylinder appears at $Z = 0$ and $\theta = 180°$, while the minimum value appears at $Z = 1$ and $\theta = 0°$. The maximum and minimum Nu_o for the outer cylinder appear at just the opposite positions to that for the inner cylinder.

Figure 5 shows the effect of R_o on local Nusselt numbers. Nu_o increases with increasing θ and Z, while Nu_i increases with decreasing Z. Such variations will be more obvious as R_o increases. Figure 6 shows the effect of aspect ratio, A, on Nu_i and Nu_o. The end effect on the inner and outer local Nusselt numbers decreases as aspect ratio increases.

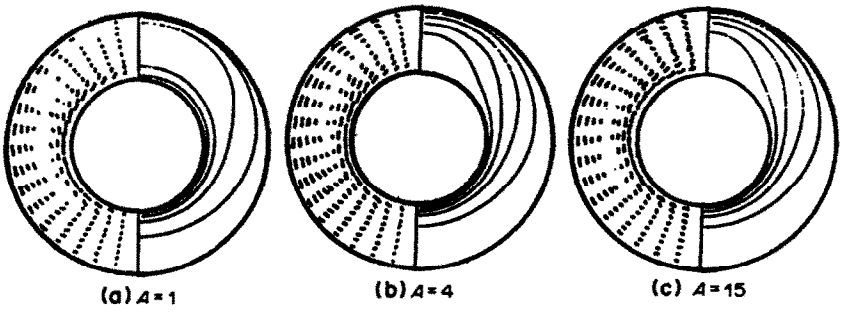

FIG. 2. Velocity fields and isotherms for the case: $Ra = 100$, $R_o = 2$, $\phi = 45°$ and $Z = 0.5$.

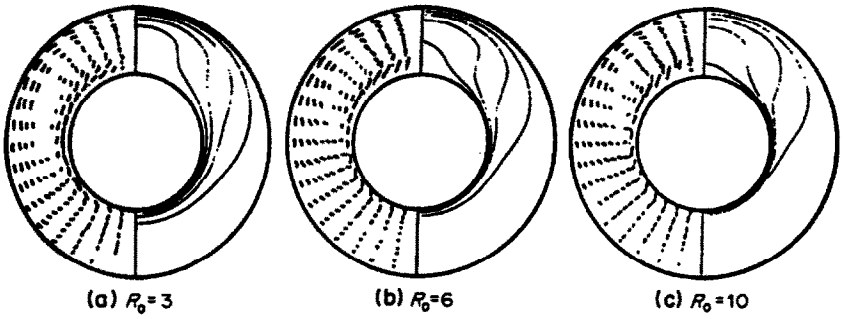

FIG. 3. Effect of radius ratio, R_o, on the velocity field and the isotherms for the case: $Ra = 100$, $A = 4$, $\phi = 30°$ and $Z = 0.5$.

Figure 7 shows the mutual effects of aspect ratio, A, and angle of inclination, ϕ, on the mean Nusselt number for the inner cylinder, $Nu_{m,i}$. We note that $Nu_{m,i}$ decreases as ϕ increases for $A > 4$, and then increases as ϕ increases for $A < 4$. So, there exists a critical aspect ratio, A_{cr}, for which the angle of inclination ϕ has no effect on heat transfer. Numerical calculation further shows that A_{cr} will decrease with increasing R_o and Rayleigh number has no effect on the critical aspect ratio.

4. EXPERIMENTAL CHECK

The experimental apparatus is designed and set up, as reported in refs. [3, 6], to conduct experiments for checking numerical results for natural convection in a

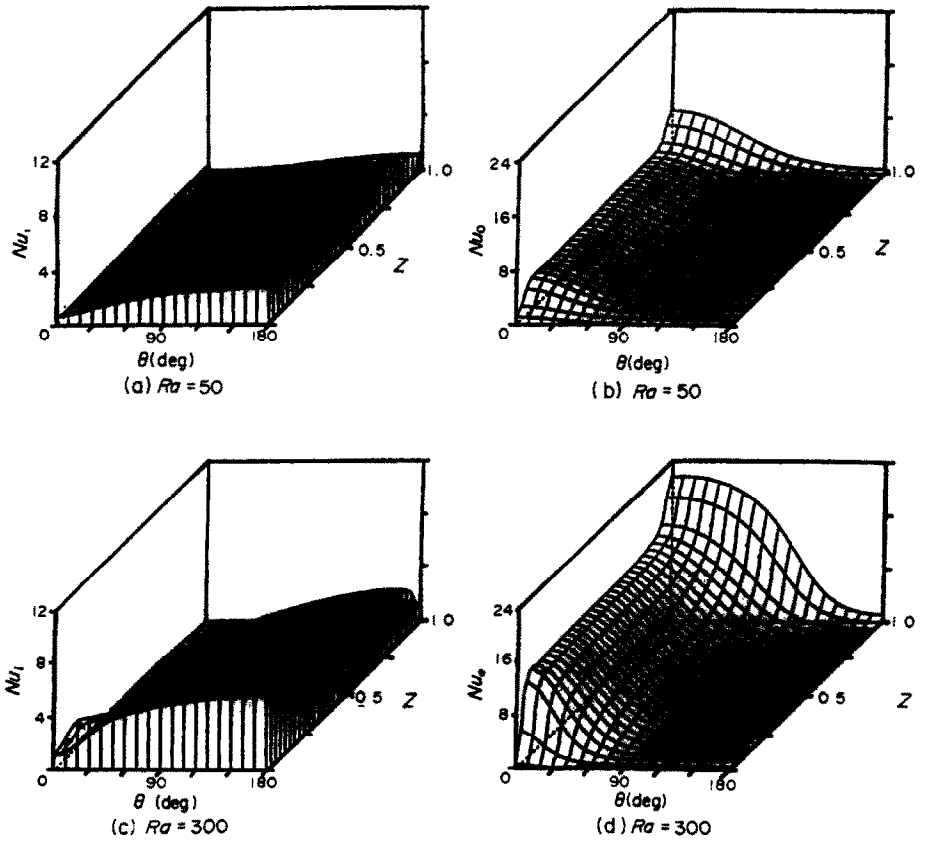

FIG. 4. The effect of Ra on local Nusselt numbers, Nu_i and Nu_o, for the case: $R_o = 5$, $A = 14.6$ and $\phi = 30°$.

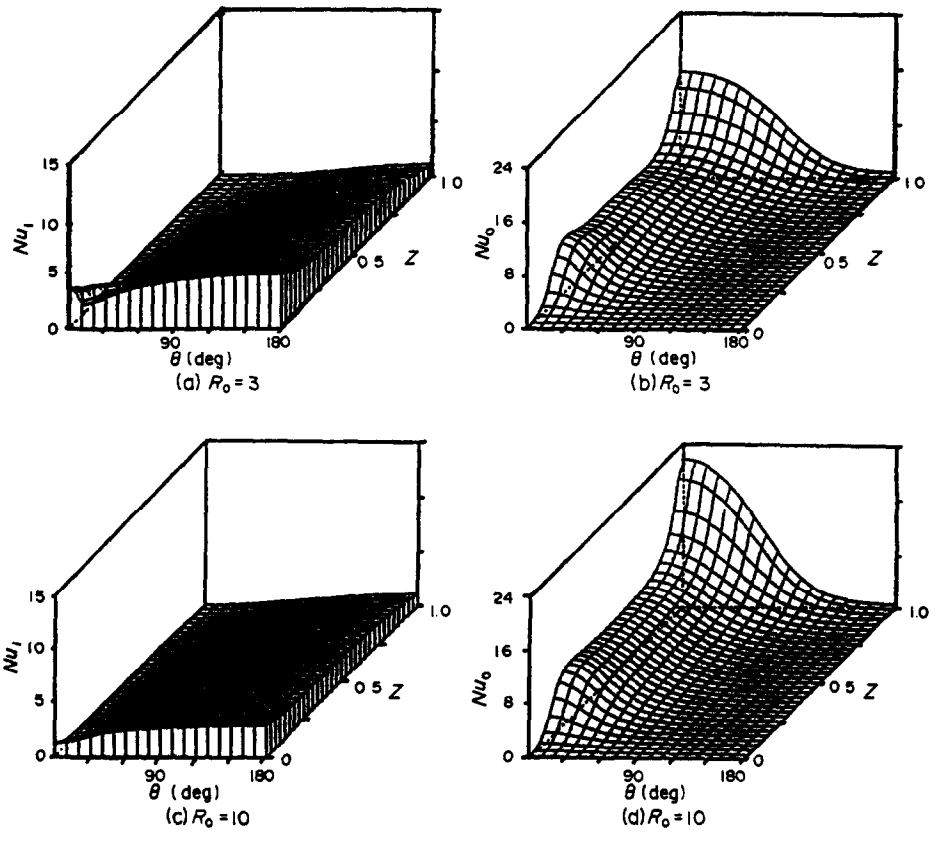

FIG. 5. The effect of radius ratio, R_o, on Nu_i and Nu_o for the case: $Ra = 100$, $A = 4$ and $\phi = 30°$.

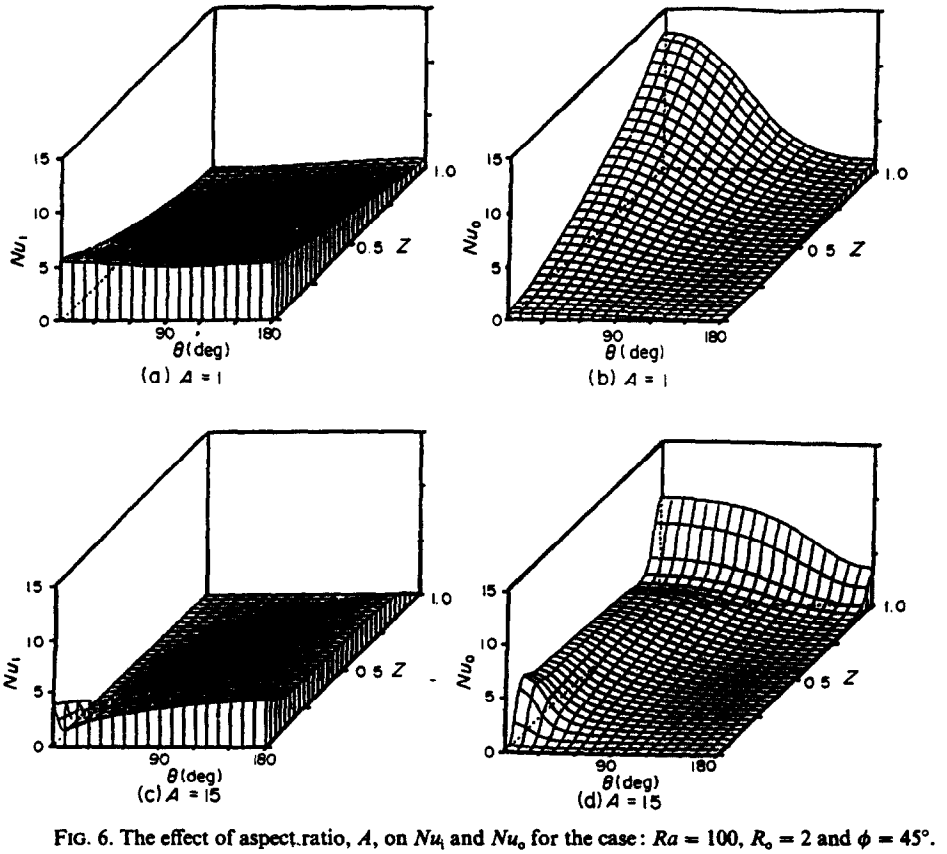

FIG. 6. The effect of aspect ratio, A, on Nu_i and Nu_o for the case: $Ra = 100$, $R_o = 2$ and $\phi = 45°$.

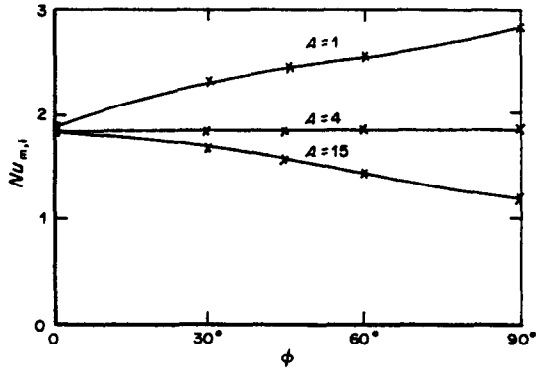

FIG. 7. The mutual effects of aspect ratio and angle of inclination on $Nu_{m,i}$ for the case: $Ra = 100$ and $R_o = 2$.

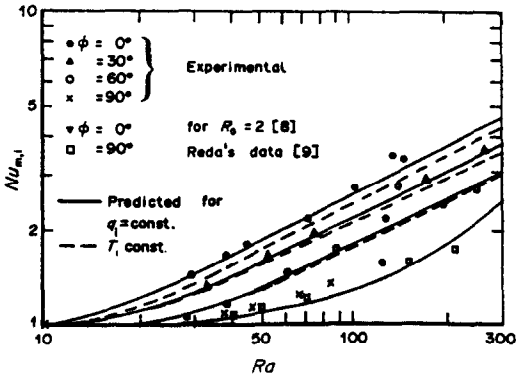

FIG. 9. The effects of Ra and angle of inclination, ϕ, on $Nu_{m,i}$ for the case: $R_o = 5$ and $A = 14.6$.

vertical ($\phi = 90°$) and in a horizontal ($\phi = 0°$) liquid-saturated porous annulus, respectively. The same apparatus was used to obtain experimental data for $\phi = 30°, 45°$ and $60°$ also. The outer cylinder was kept isothermal, T_o = const., while the inner cylinder was heated uniformly with constant heat flux, q_i.

Figure 8 shows the measured $Nu_{m,i}$ compared with numerically predicted values for the case: $A = 3$ and $R_o = 5$. Since $A = 3$ is near A_{cr}, which will decrease from 4 for $R_o = 2$ with increasing R_o, measured values of $Nu_{m,i}$ make clear that the angle of inclination, ϕ, does not affect $Nu_{m,i}$. However, as shown in Fig. 9, for the case $A = 14.55$ and $R_o = 5$, i.e. $A > A_{cr}$, ϕ affects $Nu_{m,i}$, such that the mean Nusselt number for the inner cylinder decreases with an increase in the angle of inclination. The measured values agree with the predicted values quite well as shown in both Figs. 8 and 9.

5. CONCLUSIONS

Numerical and experimental results obtained for natural convection in an inclined liquid-saturated porous annulus can be summarized as follows.

(1) Mean Nusselt numbers, $Nu_{m,i}$ and $Nu_{m,o}$, always increase with an increase in Ra for any angle of inclination.

(2) Both Nu_i and Nu_o vary with θ and Z. For $0° < \phi < 90°$, the maximum value of Nu_i for the inner cylinder and the minimum value of Nu_o for the outer cylinder appear at $\theta = 180°$ and $Z = 0$; the minimum value of Nu_i for the inner cylinder and the maximum value of Nu_o for the outer cylinder appear at $\theta = 0°$ and $Z = 1$.

(3) There exists a critical aspect ratio, A_{cr}, for which the angle of inclination, ϕ, has no effect on heat transfer. For $A < A_{cr}$, the mean Nusselt number, Nu_i, increases with an increase in angle of inclination. For $A > A_{cr}$, Nu_i decreases as ϕ increases. We find that the critical aspect ratio decreases as radius ratio increases and Rayleigh number has no effect on A_{cr}. This discovery supported by both numerical and experimental data will be valuable to clarify the actual effect of ϕ on the natural convection in an inclined liquid-saturated porous annulus.

(4) The effects of θ and Z on the local Nusselt number at the outer cylinder, Nu_o, increase as the radius ratio, R_o, increases, while the effect of Z on Nu_i for the inner cylinder decreases with an increase in the radius ratio.

(5) Experiments have been carried out to check the numerical results. The measured values for mean Nusselt numbers on the inner cylinder, Nu_i, agree with the numerical values quite well for the entire range of Ra and ϕ studied.

Acknowledgement—Project supported by Science Fund (1988–1990) from China State Commission of Education.

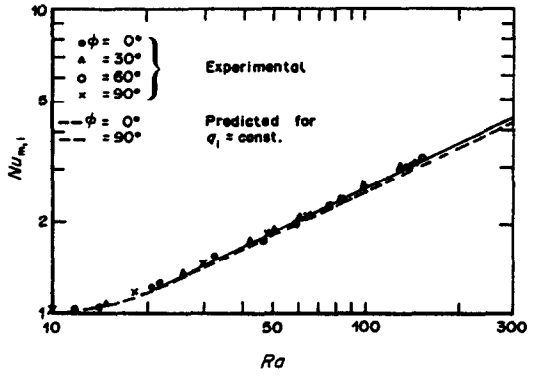

FIG. 8. $Nu_{m,i} = f(Ra)$ for the case: $R_o = 5$ and $A = 3$.

REFERENCES

1. M. A. Cambarnous and S. A. Bories, Hydrothermal convection in saturated porous media. In *Advances in Hydroscience*, Vol. 10, pp. 231–307. Academic Press, New York (1975).

2. P. Cheng, Heat transfer in geothermal systems. In *Advances in Heat Transfer* (Edited by T. F. Irvine, Jr. and J. P. Hartnett), Vol. 14, pp. 1–105. Academic Press, New York (1978).
3. B. X. Wang and X. Zhang, Numerical and experimental investigations on transient and steady-state natural convection in a vertical liquid-saturated porous annulus. In *Heat Transfer Science & Technology 1988* (Edited by B. X. Wang), pp. 417–423. Hemisphere, New York (1989).
4. Y. Takata, K. Iwashige, K. Fukuda, S. Hasegawa, H. Shimoura and K. Sanokata, Three-dimensional natural convection in porous medium enclosed with concentric inclined cylinders, *Proc. 7th Int. Heat Transfer Conf.*, pp. 351–356 (1982).
5. Y. Takata, K. Iwashige, K. Fukuda and S. Hasegawa, Three-dimensional natural convection in an inclined cylindrical annulus, *Int. J. Heat Mass Transfer* **27**, 747–754 (1984).
6. B. X. Wang and X. Zhang, Transient natural convection in a horizontal liquid-saturated porous-media annulus (in Chinese), *Chinese J. Engng Thermophys.* **10**(3), 287–292 (1989).
7. X. Zhang, Numerical and experimental investigations on three-dimensional transient and steady-state natural convection in a liquid-saturated porous annulus, Dissertation for Dr.-Eng. degree, Tsinghua University, Beijing (October 1988).
8. J. P. Caltagirone, Thermoconvective instabilities in a porous medium bounded by two concentric horizontal cylinders, *J. Fluid Mech.* **76**(2), 337–362 (1976).
9. D. C. Reda, Natural convection experiments in stratified liquid-saturated porous medium, *Trans. ASME*, Ser. C, *J. Heat Transfer* **108**, 660–666 (1986).

CONVECTION NATURELLE DANS DES MILIEUX POREUX SATURES DE LIQUIDE ENTRE CYLINDRES CONCENTRIQUES INCLINES

Résumé—On étudie numériquement la convection naturelle permanente dans un milieu poreux saturé de liquide entre des cylindres concentriques inclinés. Le cylindre intérieur est maintenu à flux thermique ou à température uniforme, tandis que le cylindre externe est isotherme et que les extrémités planes sont isolées. Les études numériques concernent: nombre de Rayleigh, $Ra \leqslant 10^3$; rapport des rayons $1 \leqslant R_o \leqslant 10$; rapport de forme $1 \leqslant A \leqslant 15$; angle d'inclinaison ϕ de 0° à 90°. Les résultats montrent qu'il existe un rapport de forme critique pour lequel l'angle d'inclinaison n'a pas d'effet sur le transfert de chaleur. On trouve un bon accord entre les calculs et les données expérimentales pour le nombre de Nusselt moyen, Nu_m.

NATÜRLICHE KONVEKTION IN FLÜSSIGKEITSGESÄTTIGTEN PORÖSEN MEDIEN ZWISCHEN KONZENTRISCHEN GENEIGTEN ZYLINDERN

Zusammenfassung—Es wird über die numerische Untersuchung der dreidimensionalen stationären natürlichen Konvektion in flüssigkeitsgesättigten porösen Medien zwischen konzentrischen geneigten Zylindern berichtet. Der innere Zylinder wird entweder mit konstanter Wärmestromdichte beaufschlagt, oder er ist auf konstanter Temperatur, während der äußere Zylinder stets isotherm und die Endflächen ideal isoliert sind. Die numerischen Untersuchungen decken folgende Bereiche ab: Rayleigh-Zahl, $Ra \leqslant 10^3$; Radienverhältnis, $1 \leqslant R_o \leqslant 10$; Seitenverhältnis, $1 \leqslant A \leqslant 15$; Neigungswinkel, $0° \leqslant \phi \leqslant 90°$. Es ergibt sich ein kritisches Seitenverhältnis, bei dem der Neigungswinkel keinen Einfluß auf den Wärmeübergang hat. Bei mittlerer Nusselt-Zahl, Nu_m, stimmen die numerischen Ergebnisse gut mit experimentellen Werten überein.

ЕСТЕСТВЕННАЯ КОНВЕКЦИЯ В НАСЫЩЕННЫХ ЖИДКОСТЬЮ ПОРИСТЫХ СРЕДАХ МЕЖДУ НАКЛОННЫМИ КОНЦЕНТРИЧЕСКИМИ ЦИЛИНДРАМИ

Аннотация—Численно исследуется трехмерная стационарная естественная конвекция в насыщенных жидкостью пористых средах, заключенных между наклонными концентрическими цилиндрами. На внутреннем цилиндре поддерживается постоянный тепловой поток или он является изотермическим, внешний же цилиндр изотермичен, а торцы теплоизолированы. Анализ проводился в диапазонах знажений числа Рэлея $Ra \leqslant 10^3$, отношения радиусов $1 \leqslant R_o \leqslant 10$, отношения длины цилиндра к величине зазора $1 \leqslant A \leqslant 15$ и угла наклона ϕ от 0° до 90°. Численные результаты указывают на наличие критического значения Λ, при котором угол наклона не влияет на теплоперенос. Получено хорошее соответствие между расчетными и экспериментальными значениями для среднего числа Нуссельта Nu_m.